Journal of Structural Geology 56 (2013) 89–102

Contents lists available at ScienceDirect

Journal of Structural Geology

journal homepage: www.elsevier.com/locate/jsg

Transtensional folding

Haakon Fossen [a, *], Christian Teyssier [b], Donna L. Whitney [b]

[a] Department of Earth Science, Museum of Natural History, University of Bergen, Postboks 7803, N-5007 Bergen, Norway
[b] Department of Earth Sciences, University of Minnesota, Minneapolis, MN 55455, USA

ARTICLE INFO

Article history:
Received 19 July 2013
Received in revised form
3 September 2013
Accepted 11 September 2013
Available online 20 September 2013

Keywords:
Transtension
Folding
Shear zones
Oblique divergence
Constrictional strain

ABSTRACT

Strain modeling shows that folds can form in transtension, particularly in simple shear-dominated transtension. Folds that develop in transtension do not rotate toward the shear zone boundary, as they do in transpression; instead they rotate toward the divergence vector, a useful feature for determining past relative plate motions. Transtension folds can only accumulate a fixed amount of horizontal shortening and tightness that are prescribed by the angle of oblique divergence, regardless of finite strain. Hinge-parallel stretching of transtensional folds always exceeds hinge-perpendicular shortening, causing constrictional fabrics and hinge-parallel boudinage to develop.

These theoretical results are applied to structures that developed during oblique continental rifting in the upper crust (seismic/brittle) and the ductile crust. Examples include (1) oblique opening of the Gulf of California, where folds and normal faults developed simultaneously in syn-divergence basins; (2) incipient continental break-up in the Eastern California-Walker Lane shear zone, where earthquake focal mechanisms reflect bulk constrictional strain; and (3) exhumation of the ultrahigh-pressure terrain in SW Norway in which transtensional folds and large magnitude stretching developed in the footwall of detachment shear zones, consistent with constrictional strain. More generally, folds may be misinterpreted as indicating convergence when they can form readily in oblique divergence.

1. Introduction

Transpression and transtension are simple 3D strain models that capture the range of possible deformation between wrenching (vertical simple shear) and pure contraction or extension (e.g., Sanderson and Marchini, 1984; Fossen et al., 1994). Transpressional deformation involves pure shear related horizontal shortening across the shear zone; hence the pure shear component promotes folding of horizontal layers (e.g., Tikoff and Peterson, 1998). For the less studied case of transtension, however, the pure shear component imposes horizontal extension across the zone and vertical shortening, and this counteracts folding. Nevertheless, as explored in this paper, folding of horizontal layers is predicted for any case of transtension (see also Venkat-Ramani and Tikoff, 2002). Our results guide the interpretation of tectonic zones in which transtension folds horizontal crustal layers during basin development (such as during oblique extension associated with rifting) or during the exhumation of deep crust (oblique orogenic extension/collapse).

2. Approach and brief theoretical background

A number of models have been put forward for transpression and transtension, including orthogonal transpression/transtension where the shear plane is vertical relative to horizontal and vertical coaxial strain axes (Fossen and Tikoff, 1998) and more complex models where the shear plane is inclined (triclinic transpression/transtension; Robin, 1994; Jones et al., 2004; Fernandez and Diaz-Azpiroz, 2009). The approach taken here is that of a theoretical study of a vertical shear zone based on the relatively simple but robust model for transpression and transtension suggested by Sanderson and Marchini (1984) and the deformation matrix presented by Fossen and Tikoff (1993):

$$D = \begin{bmatrix} 1 & \Gamma & 0 \\ 0 & k & 0 \\ 0 & 0 & k^{-1} \end{bmatrix} = \begin{bmatrix} 1 & \frac{\gamma(1-k)}{\ln(k^{-1})} & 0 \\ 0 & k & 0 \\ 0 & 0 & k^{-1} \end{bmatrix} \quad (1)$$

In this model, which has shown to capture essential aspects of transpression and transtension (e.g., Fossen and Tikoff, 1993, 1998; Jones et al., 2004; Tikoff and Teyssier, 1994), a pure shear acts in the plane perpendicular to the shear zone. For transtension, this

* Corresponding author. Tel.: +47 97018795.
E-mail addresses: haakon.fossen@geo.uib.no, haakonfossen@mac.com (H. Fossen).

0191-8141/$ – see front matter © 2013 Elsevier Ltd. All rights reserved.
http://dx.doi.org/10.1016/j.jsg.2013.09.004

involves vertical shortening balanced by horizontal extension (Fig. 1). Based on this matrix we calculate (1) the instantaneous stretching axes (ISA), notably the instantaneous shortening direction (ISA_{min}) in the plane of bedding (the horizontal plane in Sections 4 and 5), (2) the flow apophyses, (3) the rotation of material lines, and (4) the kinematic vorticity W_k (e.g., Fossen and Tikoff, 1993; Tikoff and Fossen, 1993), which varies from 1 for ideal wrenching (simple shear) to 0 for pure shear. The W_k number, which describes the noncoaxiality or the relative amount of simple versus pure shear involved, is directly related to the flow apophyses or angle (α) of divergence (for transtension; see Fig. 1) or convergence (for transpression) across the zone (Fig. 2a). Hence W_k and the angle of divergence (α) (angle of convergence for transpression) both describe the degree of noncoaxiality of transtension and transpression. In our model, a constant W_k deformation history means that one vertical boundary diverges or converges along a straight and constant displacement path relative to the other vertical boundary, i.e., the divergence or convergence vector remains constant. This makes constant W_k paths very realistic reference models for progressive transtension and transpression. For all cases, the divergence/convergence vector is parallel to the one horizontal flow apophysis that is oblique to the shear zone, while the other horizontal apophysis always parallels the shear zone. These two flow apophyses coincide for simple shear, in which case the angle of divergence/convergence is zero (Fig. 2a, lower right corner). Since transpression and transtension are three-dimensional deformations, there are three ISAs; two in the horizontal plane (ISA_{Hmax} and ISA_{Hmin}; Fig. 2b) and one vertical. The flow apophyses maintain their orientations with respect to the shear zone throughout a steady-state deformation, and these orientations depend on W_k (Fig. 2b).

In contrast, the principal strain axes (*X*, *Y*, *Z*) rotate and may switch positions during the course of deformation if the deformation is simple shear-dominated transpression or transtension ($W_k > 0.81$; Fossen and Tikoff, 1993). For simple shear-dominated transtension the minimum horizontal strain axis is *Z*, but if the strain path hits the Flinn diagram ordinate (pure constriction), the minimum horizontal axis becomes *Y*. This switch in *Z* and Y is most common for simple shear-dominated deformations close to $W_k \sim 0.85$. The maximum horizontal strain axis is always *X* for any type of transtension.

The folding considered in this paper is that resulting from layer-parallel shortening, i.e. buckle folds rather than passive folds or forced folds. For simplicity we neglect any pre-buckling layer-parallel shortening and assume that folds initiate instantaneously at the onset of layer-parallel shortening. In concert with these simplifications we make the common assumption that, for horizontal layers, fold hinges initiate perpendicular to the maximum horizontal instantaneous shortening direction (ISA_{min}) (e.g., Treagus and Treagus, 1981); this assumption is supported by numerical and experimental modeling (James and Watkinson, 1994; Tikoff and Peterson, 1998; Venkat-Ramani and Tikoff, 2002). For steady-state simple shearing, ISA_1 is always oriented at 45° to the shear zone, and the strain ellipsoid as well as folds that result from shortening rotate toward the shear plane.

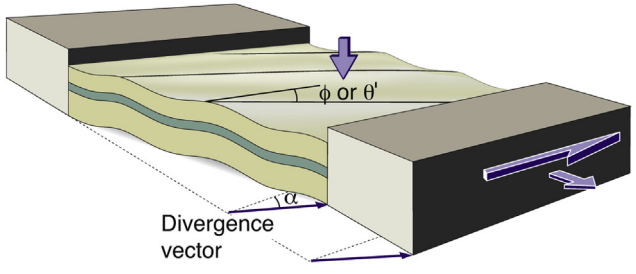

Fig. 1. Transtension in a ductile volume of rocks with horizontal layering between two rigid blocks. Deviation from simple shear is reflected by α, the angle of divergence, which is related to the kinematic vorticity W_k (Fig. 2). "ϕ and θ' refers to hinge orientation according to the passive line rotation model and the max horizontal strain axis rotation model, respectively (see text for details).

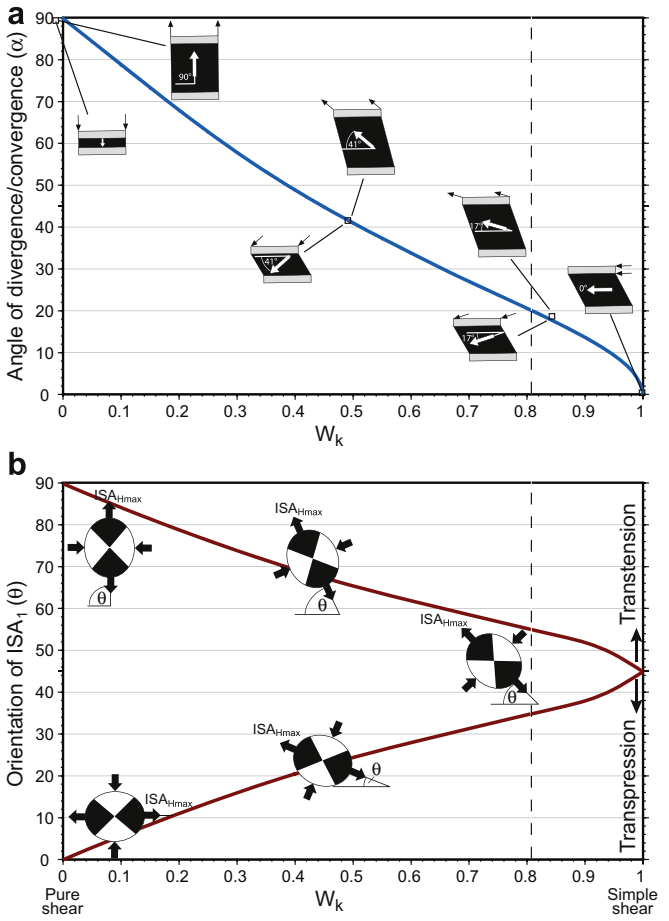

Fig. 2. a) Relationship between the angle of divergence (α) and the kinematic vorticity number W_k. The divergence vector is indicated in black boxes above the curve, and for transpression below the curve. b) Variation of ISA_1 (fastest instantaneous stretching direction) and W_k.

Exactly how fold elements (axis, axial plane) rotate after initiation is not clear. Two reference models are considered: 1) fold axes rotate as passive line markers (material lines); or 2) fold axes rotate along with the *X*-axis of the horizontal strain ellipse. In the second model material moves through the hinge, whereas in the first model the line of particles (mineral grains) along the initial hinge line will always define the hinge line. Model 2 is consistent with observations of fold rotation in transtension experiments performed on plasticine and silicone (Venkat-Ramani and Tikoff, 2002). These physical models cover simple-shear or close to simple shear-dominated transtension ($W_k > 0.81$ or $\alpha < 20°$). More data from physical experiments, numerical modeling and field observations are needed to further explore this question.

The difference between the two reference models of hinge rotation relates to the fact that material lines rotate faster than theoretical strain axes for low to moderate strains, and this difference in rotation rate increases with increasing degree of noncoaxiality (increasing W_k). At higher strains the theoretical strain axes rotate faster, and at infinitely high strain the amount of finite

hinge rotation is identical for the two models. In this work, where we explore the full spectrum of oblique divergence cases through a theoretical approach, we consider the rotation of a fold hinge as tracking either the strain axis or a material line. The passive line marker rotation (model 1) can be calculated from the deformation matrix (Eq. (1)) through the linear transformation:

$$\mathrm{l}' = \mathrm{Dl} \tag{2}$$

where l and l' are the initial and new orientations, respectively, of a unit vector along the fold axis, and **D** is the deformation matrix from Equation (1). Rotation of the long axis of the strain ellipse in the horizontal plane (model 2) is described by the equation

$$\theta' = \tan^{-1}[(\lambda - \Gamma - 1)/\mathrm{k}\Gamma] \tag{3}$$

where θ' is the angle between the maximum horizontal principal strain axis (X for transtension) and the shear direction.

We use the kinematic vorticity number W_k and the angle of divergence (α) (angle of convergence for transpression) to describe the degree of noncoaxiality (Fig. 2). The angle α is also the angle between the oblique flow apophysis and the x-axis, and is given by the formula

$$\alpha = \tan^{-1}[\ln(\mathrm{k})/\lambda] \tag{4}$$

Thus, the relative components of pure and simple shear deformation can be described by either W_k or the convergence/divergence angle (α) of the system. In the following two sections we briefly revisit simple shear and transpression before discussing strain and folding in transtension.

3. Simple shear

Simple shear is a convenient reference model for shear zones, and it also defines the boundary between transpression and transtension in terms of strain and kinematics. Hence we find it useful to briefly review folding of initially horizontal layers in a vertical simple shear zone before exploring transtension folding.

For horizontal layers, simple shear-generated folds initiate close to 45° to the shear zone boundary. As deformation proceeds, folds rotate toward the shear direction (horizontal flow apophysis) so that the sector of hinge rotation approaches 45° (Fig. 3a). This simple shear rotation is also shown in Fig. 4 for the two models of hinge rotation represented by the thick blue line starting at $\phi = 45°$. In Fig. 4a (model 1) the orientation of the line (presumed fold hinge line) that initially forms perpendicular to $\mathrm{ISA}_{\mathrm{min}}$ is plotted against the finite shortening in the horizontal plane (minimum horizontal principal strain, Z for simple shear). As an example, the graph shows that after 30% shortening of the horizontal layer, the fold axis has rotated from 45° to 30°. The amount of shortening is visualized by the shape of folded layers along the abscissa axis of Fig. 4. Fig. 4b shows the same set of curves for model 2, where fold hinge rotation tracks the maxium horizontal finite strain axis (X for simple shear). The simple shear curve now has a more convex shape, which reflects the fact that passive material lines (Fig. 4a, model 1) rotate faster at low strain and slower at high strain than the theoretical X-axis of the strain ellipsoid (Fig. 4b, model 2). Using the same example as above, the orientation of the fold axis after 30% shortening is now 35°, i.e. the rotation is 5° less than for model 2.

4. Transpression

Transpression is created by adding pure shear in the form of shortening perpendicular to the shear zone compensated by vertical extension. The amount of pure shear relative to simple shear is expressed by the kinematic vorticity number (W_k) or the angle of convergence (α).

For transpression the initial orientation of fold axes in horizontal layers is $< 45°$, and the rotation is less than for simple shear by an amount that depends on α or W_k (Fig. 4). The shaded sectors in Fig. 3e–g show the full range of possible rotation of horizontal lines (fold axes) for a few cases. The rotation sector shrinks as W_k decreases (and as α increases), from 45° for simple shear to 0° for pure shear, in which case folds form and remain parallel to the shear zone. Note that the rotation sector is limited by the maximum horizontal ISA and the shear zone, and this holds true for both rotation models.

5. Transtension

Transtension zones combine simple shear with lateral extension and vertical shortening (Fig. 1). The horizontal "pull" causes the folds to initiate at an angle higher than the 45° simple shear angle (Fig. 3b–d, 4). The fold axes rotate in the same sense as for simple shear, but the sector of rotation decreases with increasing coaxiality (decreasing W_k) and increasing divergence (α). Contrary to both simple shear and transpression, the rotation sector is now limited by the maximum horizontal ISA and the oblique horizontal flow apophysis (divergence vector). Hence for transtension the folds never rotate into parallelism with the shear zone as they never rotate through the oblique flow apophysis. Note that the sector of hinge rotation (red arrow in Fig. 3) is identical for the two models: both strain X-axis and material line (fold hinges) initiate parallel to the maximum instantaneous stretching axis (ISA_1) and rotate toward the oblique flow apophysis. The amount of rotation for various values of W_k is shown in Fig. 5. However, the rate of rotation is higher for the material line rotation model (model 1) for low and intermediate strains.

5.1. Transtensional folding

The most fundamental parameter that controls folding in transtension in a shear zone with horizontal layers is the amount of shortening in the horizontal plane. This parameter is captured in Fig. 4 (abscissa) for both the material line (Fig. 4a) and strain axis rotation models (Fig. 4b). These graphs show the initial angle of fold hinges along the ordinate axis, which is different for different values of W_k but is identical for the two models. The change in hinge orientation is represented by constant W_k curves (fixed divergence vector).

While folds generated during transpression rotate toward parallelism with the shear zone boundary (toward the lower right-hand corner of Fig. 4a and b), transtensional folds rotate toward an oblique orientation that is determined by the flow apophysis (the angle α) (AP in Fig. 3b and c), i.e. the divergence vector. The lower the kinematic vorticity number, i.e. the stronger the divergent component, the less the hinge line rotates. More importantly, there is a limit in the amount of finite horizontal shortening that transtensional folds can take up (Fig. 4b). This value is plotted along the abscissa of the graph, and fold shapes are added to Fig. 4 for visualization. For example, in Fig. 4b (model 2) for $W_k = 0.5$ the shortening approaches 35% (the minimum horizontal strain axis is 0.65). Hence transtensional folds can only accumulate a fixed amount of shortening, and therefore a fixed interlimb angle. The value of this angle is, again, controlled by W_k or the degree of coaxiality (Fig. 4). Simple shear-dominated transtension can produce tight folds from horizontal layers, while pure-shear dominated transtension cannot, not even for infinitely high strains.

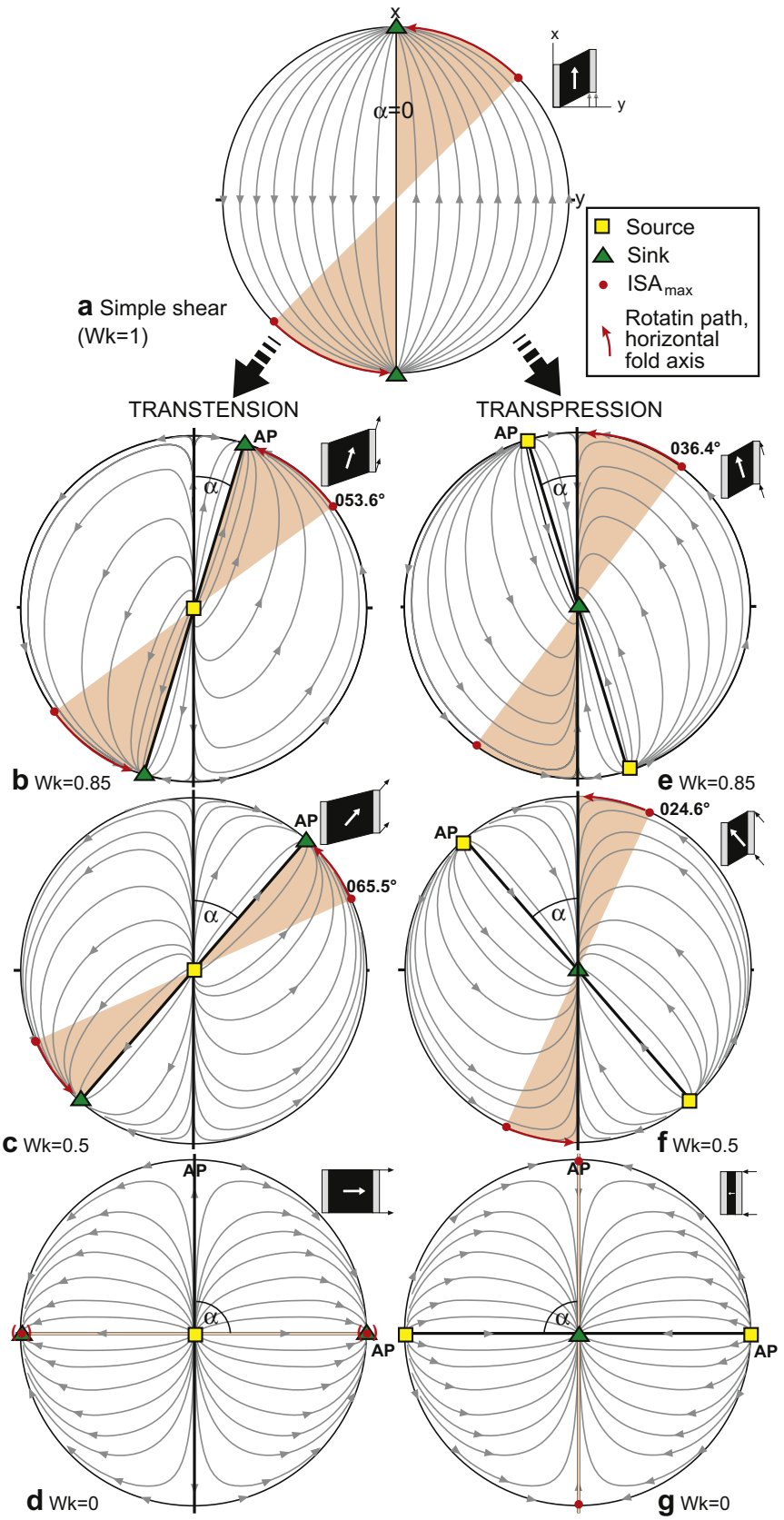

Fig. 3. Stereographic representations of passive line rotation patterns (grey) in a) simple shear. b–d) transtension, and e–g) transpression for selected values of W_k. Red points indicate initial orientation of fold hinges forming in horizontal layers, and the arrows (and shaded fields) indicate fold axis rotation with increasing strain. (For interpretation of the references to color in this figure legend, the reader is referred to the web version of this article.) Based on Fossen et al. (1994).

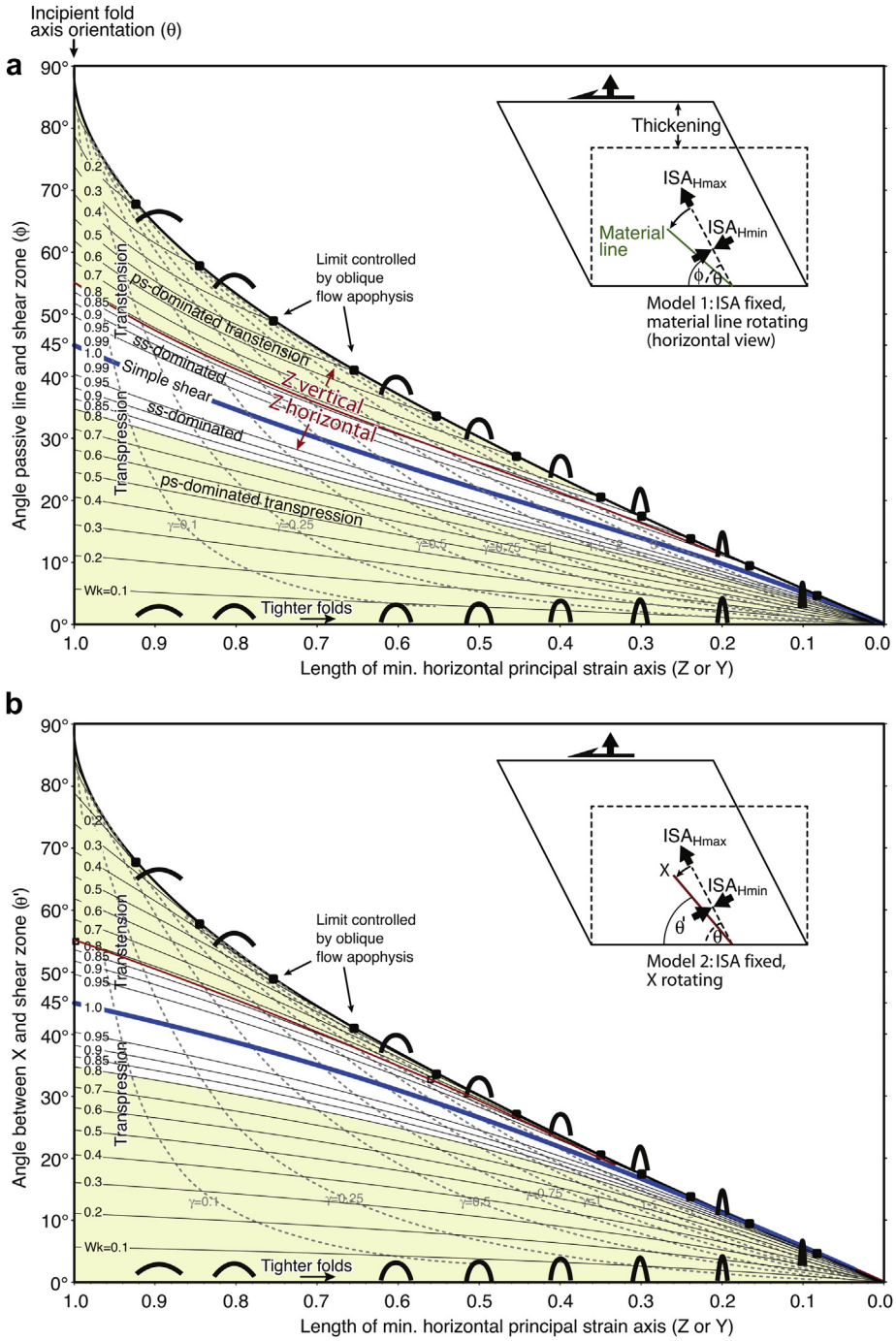

Fig. 4. Graph of change in orientation of folds from their initial orientation (where curves intersect the ordinate) for various values of W_k. a) fold hinges are assumed to rotate as passive lines (model 1 in the text); b) fold hinges are assumed to rotate with the largest principal strain axis *X* (model 2). The graph abscissa shows the amount of accumulated shortening (0.9 implies 10% shortening, etc.) represented by the possible tightness of folds. Transtensional deformations plot above the blue simple shear curve. Note that the field of rotation decreases with decreasing W_k value because, for transtension, both material lines and the strain *X*-axis rotate toward the oblique apophysis, not the shear direction (compare with Fig. 3). The red curve indicates pure constriction ($Z = Y$) and separates simple shear-dominated transtension (where *Z* is horizontal) from pure shear-dominated transtension (*Z* vertical). Simple shear values (γ) are shown as faint stippled lines. (For interpretation of the references to color in this figure legend, the reader is referred to the web version of this article.)

5.2. Horizontal stretching versus shortening

Stretching and shortening occur simultaneously in the horizontal plane during simple shear as well as transtension and transpression (Withjack and Jamison, 1986; Jamison, 1991; Teyssier and Tikoff, 1998). This means that stretching of the hinge is expected as transtensional folds amplify and tighten (Fig. 6). Fig. 7 shows graphs similar to those in Fig. 4, but for the maximum horizontal stretching rather than shortening. Because in transtension only the horizontal *X* strain axis is stretching, stretching along *X* is faster than the shortening along each of *Y* and *Z*. Only for simple and pure shearing is the stretching rate of *X* balanced by the shortening rate along *Z*. The other extreme occurs along the red line in Fig. 4 (pure constriction), where the rate of stretching on *X* is twice that

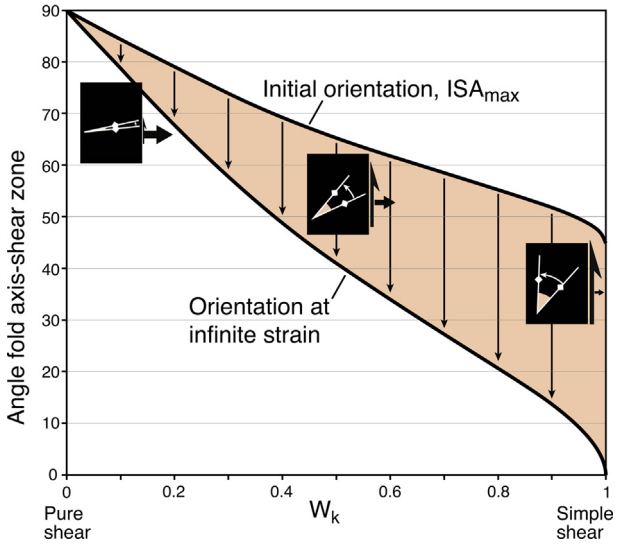

Fig. 5. The change in orientation of hinges from their initial orientation to the orientation that they approach as strain accumulates for different values of W_k (graph abscissa). There is no rotation for pure shear (left), and 45° rotation for simple shear. The amount of rotation during transtension falls between these values, depending on W_k or the relative contribution of pure and simple shear.

of Z or Y. This implies that for transpression and simple shear there is also hinge-parallel stretching during folding, but the stretching component is more pronounced for transtension, particularly if the pure shear component is strong (low W_k). Just as there is a maximum shortening value that can be achieved in transtension, there is a maximum extension value that can be reached during transpression, and that value is the intersection of W_k-curves with the graph abscissa (Fig. 7).

The relationship between simultaneous stretching and shortening in the horizontal plane is illustrated in Fig. 8, where these two parameters are plotted for various constant W_k deformations. In this graph the point A indicates that a simple shear causing 50% horizontal shortening ($Z = 0.5$) also produces 200% hinge-parallel extension ($X = 2$), i.e. $X = 1/Z$. For transtension with $W_k = 0.85$ (point B, Fig. 8) and the same amount of shortening ($Z = 0.5$) the maximum horizontal strain is now as high as 4.2, i.e. 420% hinge-parallel extension. Hence, for transtension the horizontal extension is higher than the corresponding horizontal shortening, while for transpression it is the other way around.

5.3. Three-dimensional strain

Transtension is a three-dimensional deformation that, according to the simple model applied here, generates constrictional strain. In the Flinn diagram (Fig. 9) it is shown how various constant

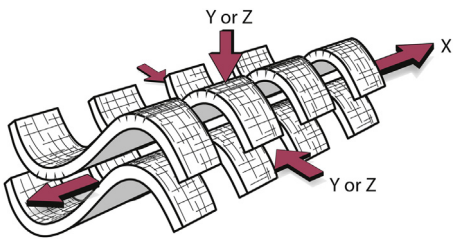

Fig. 6. Illustration of extended folds as they would appear in a wrench-transtension system. Extension could be accommodated by normal faults, veins and boudins (as shown here), or simply by layer thinning.

W_k paths are associated with the minimum horizontal strain axis (the value from the graph abscissa, Fig. 4) and strain geometry; the distance from the origin can be considered a measure of strain magnitude (Ramsay and Huber, 1983). The upper diagram (Fig. 9a) where Z is horizontal shows that the strain required for reaching a certain horizontal shortening increases with an increasing coaxial component (increasing W_k), a finding that is consistent with the conclusion from the previous subsection. For instance, the distance from the origin of the Flinn graph to the point where 30% horizontal shortening is achieved is about 2.5 times higher for $W_k = 0.81$ (point a) than for $W_k = 1.0$ (point b; simple shear) (note the logarithmic scale of Fig. 9). The difference decreases for an increased simple shear component (Fig. 9a), but for lower values of W_k (stronger influence of pure shear) the difference gets larger (Fig. 9b). Hence, in terms of strain, folding is more easily achieved for deformation closer to simple shear.

5.4. Implications for structural development

The strain produced during transtension manifests itself in ways that depend on a number of factors, including lithology, mechanical and rheological properties that may depend on pressure and temperature, and the development of strain partitioning (e.g., Tikoff and Teyssier, 1994; Krabbendam and Dewey, 1998).

The typical middle-lower crustal response to the overall constrictional strain regime that characterizes transtension is the formation of a strong linear fabric (L > S or L tectonites; Fig. 10, lower part). Hence, a pronounced stretching lineation parallel to fold hinges would be a signature of transtension at this crustal level. For certain layers with sufficiently high contrast in viscosity we may also expect to see boudinaged folds (Fig. 6), including chocolate boudinage in the hinge region if outer-arc stretching (see upper layer in Fig. 6) is substantial.

In the shallower brittle regime or near the brittle–ductile transition, ductile thinning of layers would be viable only in sediments or poorly consolidated sedimentary rocks. Instead we would expect stretching to be expressed by conjugate normal faults striking perpendicular to fold hinges (Jamison, 1991), and subvertical extension fractures and veins with a similar strike (Fig. 10, upper part).

6. Vertical layering

Some transpressional-transtensional shear zones in metamorphic rocks are subvertical with a steep foliation or layering. This situation is quite different from that of horizontal layering in several ways. It is now the vertical strain that potentially generates folds, one that is related to the coaxial strain component only. The vertical principal strain is contractional for all cases of transtension, and extensional for all cases of transpression. This implies that folds potentially form for the whole spectrum of transtensional deformations, whereas boudins (including chocolate boudins) may form during transpression since transpression strain is flattening. The two are separated by simple shear for which no vertical shortening or extension occurs. For a vertical foliation parallel to the shear zone, these folds form with horizontal axes and horizontal axial planes (Fig. 11, inset), both of which stay fixed without any rotation because there is no rotational strain in the vertical plane. Hence only fold tightness is dependent of W_k and finite strain.

Vertical shortening for transtension is not very significant if deformation is close to simple shear, but becomes much more important for pure shear-dominated transtension. As compared with the folding of horizontal layers, folding of vertical layers is more effective once the vertical principal strain becomes Z. Fig. 11

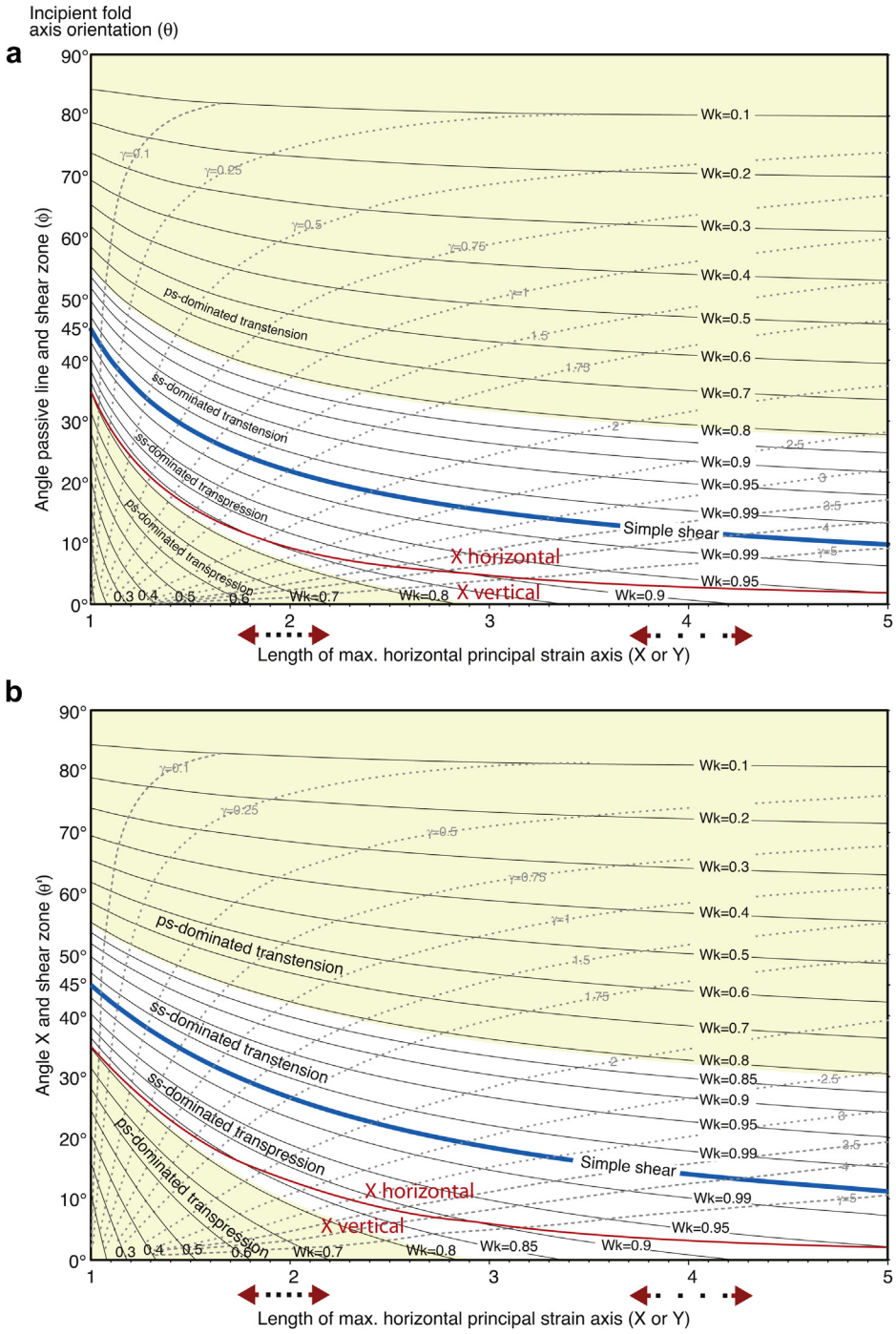

Fig. 7. Curves of fold hinge rotation for a range of W_k values for transtension upper part) and transpression (lower part) with respect to the maximum horizontal principal strain (*X* or *Y*). a) passive line rotation model. b) Hinge rotating with the largest horizontal principal strain axis. The abscissa shows the amount of accumulated stretching factor (factor of 2 implies doubling of original length, etc.).

shows this relationship, where the field beneath the diagonal depicts where *Z* is vertical and hence where vertical shortening is greater than horizontal shortening. As the simple shear-dominated transtension paths cross the diagonal in this figure the vertical strain changes from *Y* to *Z*. *Z* is always vertical for pure shear-dominated transtension paths.

The transtension model applied here produces no horizontal extension or shortening in the plane parallel to the vertical shear zone margins. This implies that a vertical layer oriented parallel to the zone margins (Fig. 11 inset) will not stretch (or shorten) in the horizontal direction, i.e. along the hinge. Hence we will not expect any hinge-parallel stretching lineation or boudinaged folds of the type portrayed in Fig. 6 for this case. However, for cases where layering is oblique to the shear zone, fold axes will stretch (or shorten, depending on the sense of shear) and rotate toward the stable position defined by the divergence vector (Fig. 3).

7. Oblique layering and progressive overprinting

Between end-member horizontal and vertical layer orientations, there is a full range of other possible layer orientations. We will not explore all of those cases here, but rather point out that it

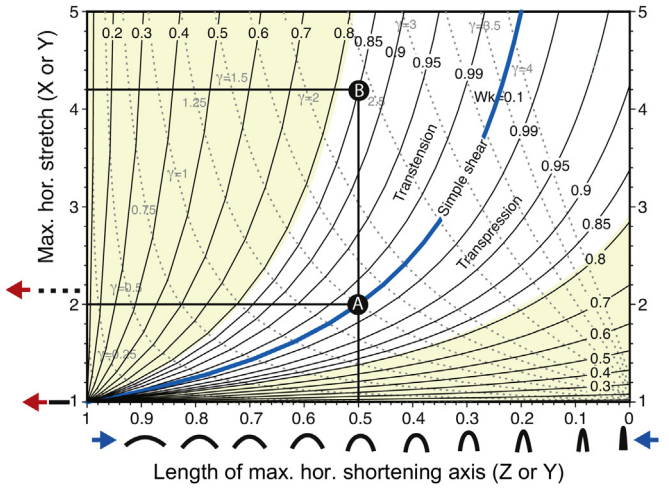

Fig. 8. Relationship between the maximum (ordinate) and minimum (abscissa) horizontal principal strain axes in transtension (upper left part) and transpression (lower right part).

may be important to consider progressive layer rotation during folding in high-strain transtensional shear zones.

For folding of initially horizontal layers the limbs steepen and thus gradually experience strain more like vertical layers do. If limbs become sufficiently steep they start to shorten and potentially buckle in the vertical direction. The result may thus be upright folds overprinted by folds with horizontal axial surfaces, as illustrated in Fig. 12a. In this case we would expect a subhorizontal secondary cleavage or axial surface overprinting upright folds. The hinges of both fold sets would be subparallel (Type 3 interference pattern of Ramsay and Huber, 1987) and oblique to the shear zone walls.

Similarly, for folding of initially vertical layers the limbs rotate toward the horizontal plane to produce a recumbent fold style (Fig. 12b). For high strains the limb may get close enough to horizontal that the shear component generates secondary folds or crenulations to the recumbent folds. A secondary vertical axial planar cleavage and/or upright folds may be the result (Fig. 12b). The two sets of fold axes will be parallel (F1) and oblique (F2) to the shear zone, where the obliqueness of F2 will be controlled by W_k and the amount of strain involved. In both these cases we generate two generations of folds during steady-state progressive folding.

8. Application to oblique tectonics: examples from brittle and ductile crust

Transtension is a deformation model applicable to tectonic zones of oblique divergence (Withjack and Jamison, 1986; Fossen et al., 1994), and therefore the strain and structure patterns predicted by transtension theory should provide insight into the interpretation of natural structures (foliation, lineation, folds, normal/detachment faults and shear zones). Oblique divergence is common at rifting plate boundaries and may characterize transtension zones along large strike-slip or transform systems, at least locally. Actively rifting plate margins commonly involve oblique divergence; examples abound and include the Gulf of California (e.g. Nagy and Stock, 2000; Aragon-Arreola et al., 2005; Umhoefer, 2011), the East African Rift (Rosendahl, 1987; Mortimer et al., 2007; Corti, 2009), the Gulf of Aden (Dauteuil et al., 2001; Leroy et al., 2012), the Gulf of Aqaba/Levant (Mart et al., 2005; Ehrhardt et al., 2005), the northern Andaman Sea (Vigny et al., 2003), and the Marmara Sea (McNeill et al., 2004).

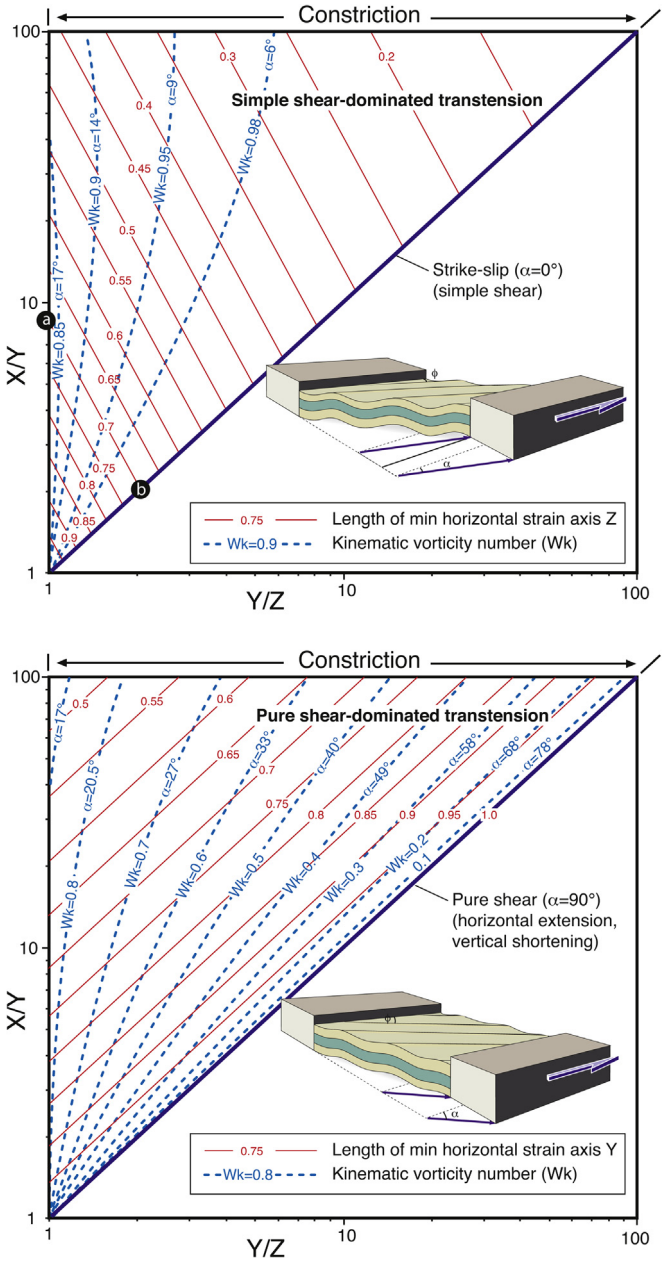

Fig. 9. Flinn diagram showing the amount of shortening (red lines) that accumulates for different constant W_k strain paths/angles of divergence (blue dashed lines). The upper diagram is for simple shear-dominated transtension; the lower diagram represents pure shear-dominated transtension. (For interpretation of the references to color in this figure legend, the reader is referred to the web version of this article.)

Oblique divergence can also occur during extension of thick and/or hot crust in cases of oblique orogenic collapse and extension. Examples include the Siluro-Devonian Norwegian Caledonides (Krabbendam and Dewey, 1998), the Cretaceous Fosdick Mountains in Antarctica (McFadden et al., 2010), the Eocene Okanogan dome (Kruckenberg et al., 2008), and the Variscan Montagne Noire, French Massif Central (Nicolas et al., 1977; Rey et al., 2011). These terrains are typically characterized by migmatite domes with associated folds and strong linear fabrics in the footwall of a detachment shear zone that grades rapidly upward into a slightly metamorphosed or non-metamorphosed upper plate (oblique metamorphic core complex).

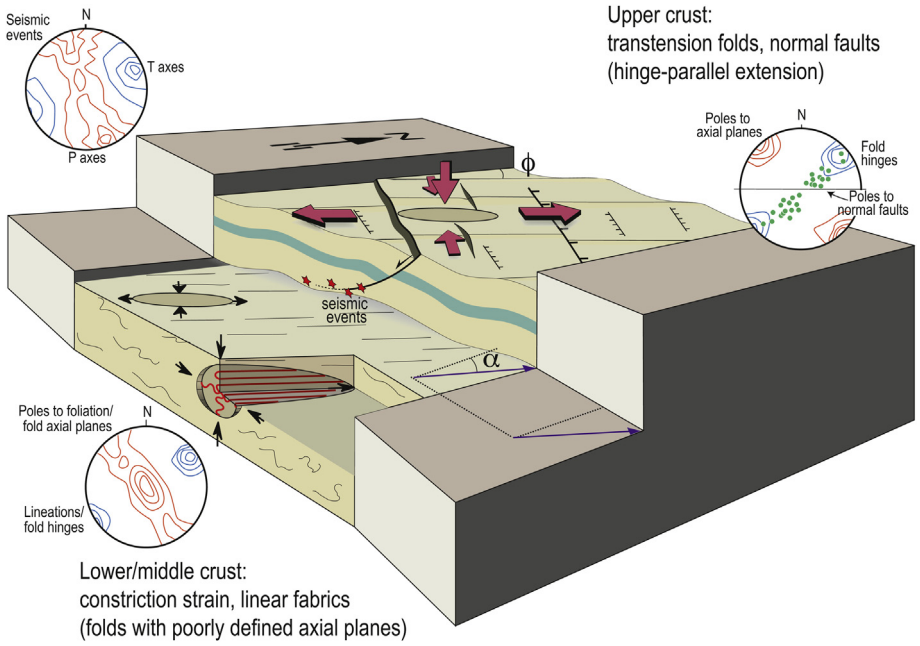

Fig. 10. 3-D illustration of transtension and related structures expected to occur in the upper and lower part of the crust. See text for discussion.

Here we use three examples to illustrate (1) the application of transtension theory to structures that form in the upper crust during oblique rifting (Gulf of California), (2) the possible seismic signature of transtension in an obliquely diverging zone of incipient continental break-up (Coso geothermal field, Eastern California transtension zone), and (3) the case where large volumes of ductile crust deform in transtension during exhumation in oblique divergence (Western Gneiss Region, Norway).

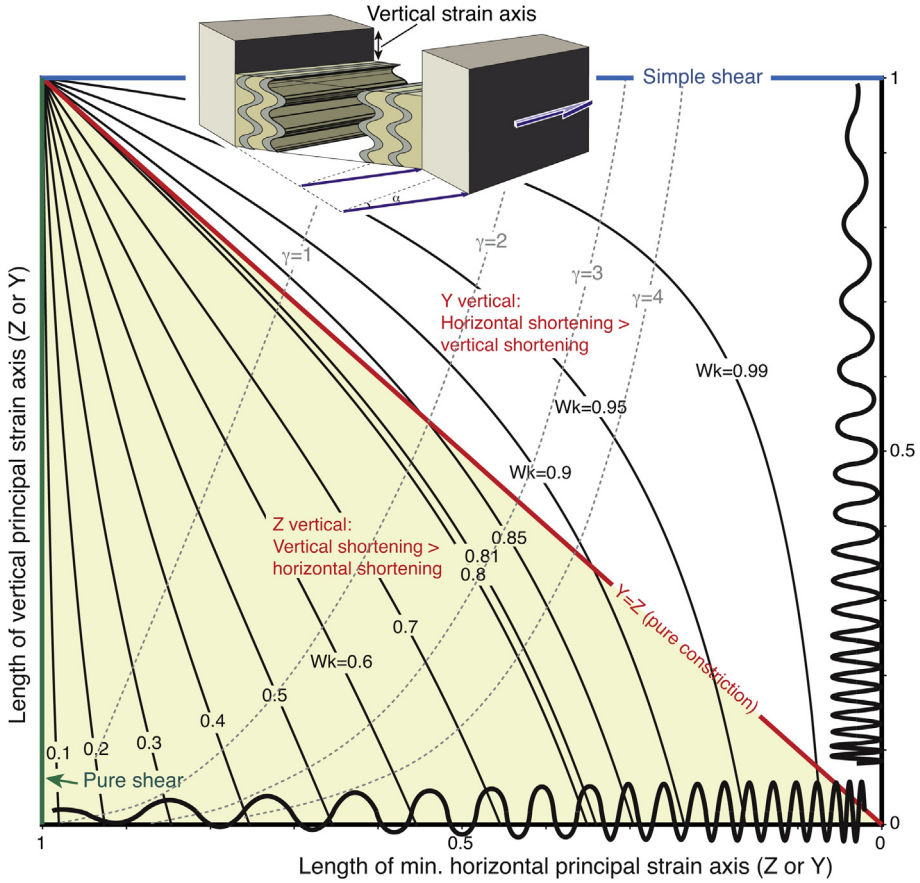

Fig. 11. Vertical principal strain axis (ordinate, *Z* or *Y*), representing vertical shortening of vertical layers, plotted against the minimum horizontal principal strain (abscissa, Y or *Z*). The diagonal marks the line where the two minimum strain axes are of the same magnitude ($Y = Z$, pure constriction). Paths of constant kinematic vorticity (W_k) are also shown.

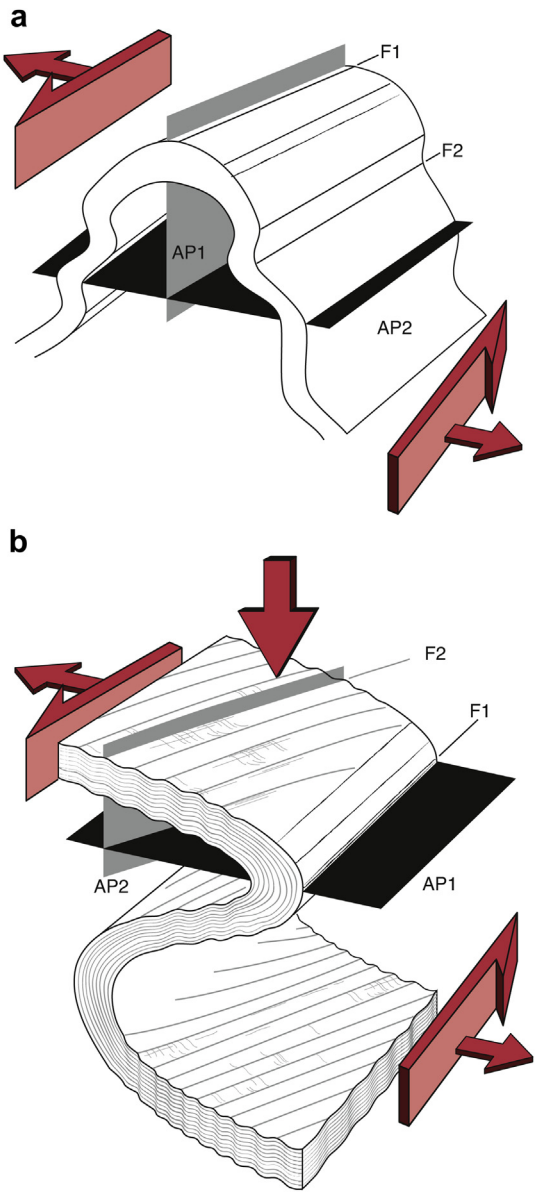

Fig. 12. Fold superposition during progressive transtension (at high strain). a) Initially horizontal layers subsequently shortened in the vertical direction as limbs steepen. b) Initially vertical layering shortened in the vertical direction. Once limbs rotate sufficiently toward a horizontal position, the shear component induces oblique folds (F2) on low-angle limbs.

8.1. Gulf of California oblique rifting (Mexico)

The Gulf of California opened rapidly during the Late Miocene, as the Pacific and North American plates diverged obliquely. Oblique rifting was first distributed in a broad zone of transtension that is well preserved on the shores of Baja California and mainland Mexico, and then localized along the axis of the gulf after ~6 Ma (Oskin et al., 2001). Strain localized along a recent volcanic arc (weak crust) that had just developed between two older and relatively rigid batholith belts (Umhoefer, 2011). The arrangement of en-échelon strike-slip faults (Lonsdale, 1989) allowed rhombochasms to develop between P-shears (Tikoff and Teyssier, 1992). These pull-apart structures focused sea-floor spreading shortly after the initiation of crustal extension (Umhoefer, 2011).

Several areas have been studied in detail in Baja California, including the Pliocene Loreto, San José Island, and related basins that may form a class of transtensional fault-termination basins (Umhoefer et al., 2007). At the northern end of the Baja California peninsula, the Sierra San Felipe and the Santa Rosa basin display strike-slip and normal faults, a low-angle detachment fault (Santa Rosa detachment), and transtensional folds (Fig. 12) that formed during the early phases of oblique divergence, around 8-9 Ma (Seiler et al., 2010). The Santa Rosa detachment affects both the Santa Rosa basin and the crystalline basement. The detachment surface is folded (megamullions) with amplitudes of 4–7 km and half wavelenths of 15–20 km (Seiler et al., 2010). According to these authors, folds of the detachment surface also occur on a smaller scale (1–2 km half-wavelength), with fold axes plunging shallowly to the E-SE. Normal faults strike nearly perpendicular to the fold hinges, as is expected from transtension (Seiler et al., 2010). This example demonstrates the coeval nature of normal faulting and the formation of fold hinges parallel to the extension direction. T and P axes derived from the kinematic analysis of small faults indicate an NW extension direction and a broad distribution of contraction axes, from shallow to steep, along a partial great circle (Fig. 13, after Seiler et al., 2010). Bulk strain accommodated by faulting and folding is consistent with constriction.

8.2. Strain and seismicity – Coso geothermal field (California)

The Gulf of California structures continue northward and connect up with the actively deforming Eastern California-Walker Lane shear zone. The Coso geothermal field is located on the western edge of this shear zone between Death Valley and the Sierra Nevada (Fig. 14a). This is a critical region that accommodates oblique motion of the rigid Sierran Block relative to North America; the motion vector is well defined by geodetic record (Dixon et al., 2000). The Coso region contains a sequence of Pliocene basaltic and andesitic lava flows that provide a rejuvenated surface, and these lava flows are tracking on-going motion and strain obtained from GPS stations. This surface also records longer term deformation that started between 3.5 and 2 Ma and is characterized by faults and folds, including the growing White Hills anticline (Fig. 14b). In a detailed and comprehensive study of the Coso field, Lewis (2007a, b) integrated results from seismicity (1000s of small magnitude events), fault-slip (slickenside) measurements, and GPS-based displacements. Some of their results are reproduced in Fig. 14; this study provides a window through a seismogenic crust that is subjected to oblique divergence, in relation to larger strain and rotation patterns that have been accommodated by surface rocks.

The Coso geothermal field region features the western Indian Wells hypocenters that can be grouped into extension-dominated and strike-slip dominated (Fig. 14b), although these two groups overlap spatially. Taken together, these seismic events define T-axes (tension-axes or minimum compressional stress direction) that are oriented nearly E-W (Fig. 14c), and P axes that are distributed on a girdle, reflecting the transtensional character of seismogenic deformation (Lewis, 2007b). Four GPS stations provide a short term direction of extension in the same region; that direction is oriented WNW-ESE (Fig. 14d). As discussed by Lewis (2007b), it is unclear what boundary orientation can be considered the “transtension shear zone” boundary against which the various strain axes can be compared. However, it is clear from this example that this incipient plate boundary is undergoing oblique rifting and that seismicity, incremental deformation, and folding can be integrated into a broad zone of oblique divergence in which block motion and strain directions are consistent with transtension (Fig. 14d).

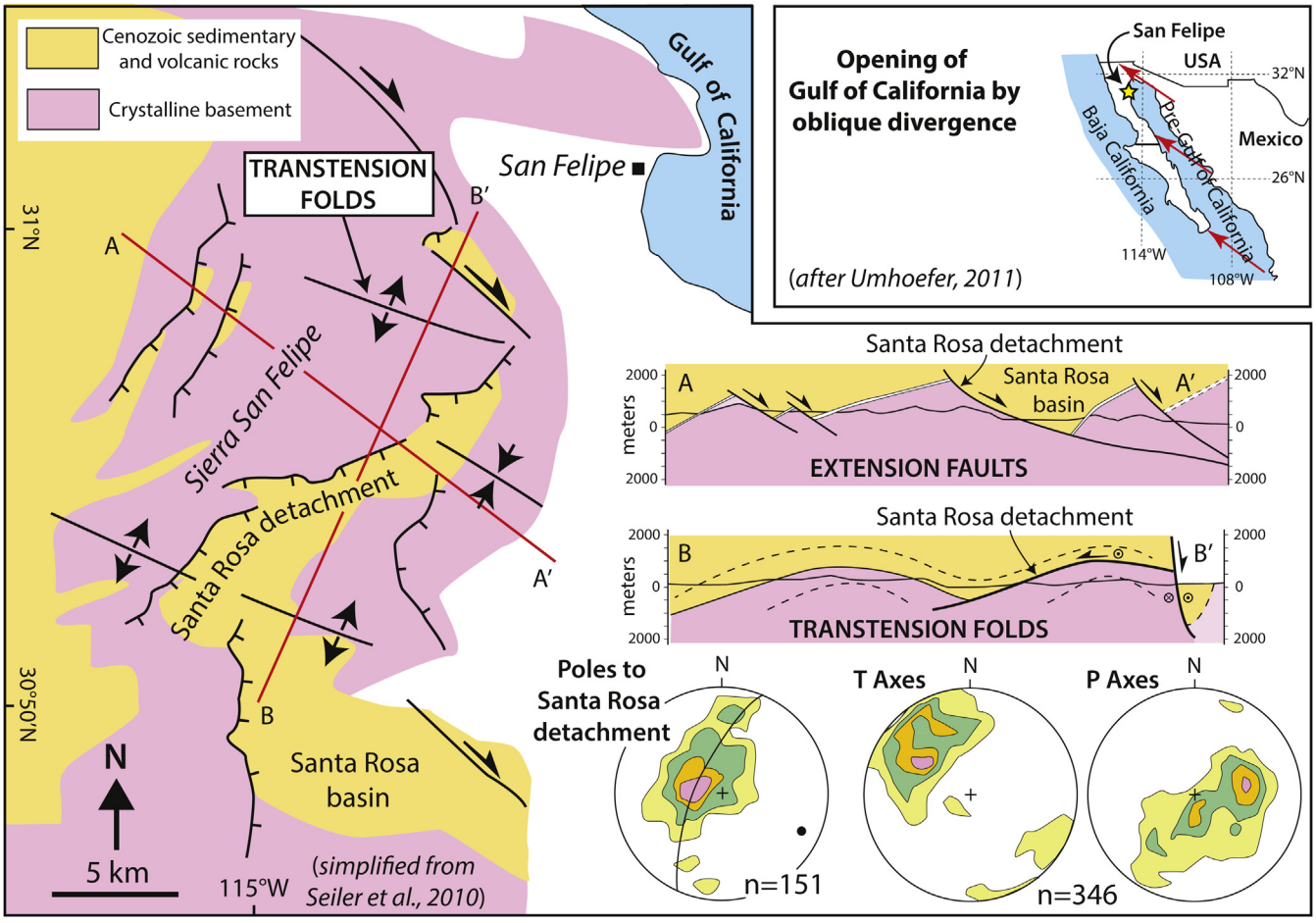

Fig. 13. Late Cenozoic oblique divergence and folding in San Felipe region, Baja California (after Seiler et al., 2010). Note detachment tectonics on cross-section A–A′ and folds wavelengths and amplitudes on cross section B–B′ (perpendicular to fold hinge). San Felipe area located on simplified map of Baja California (upper right, after Umhoefer, 2011).

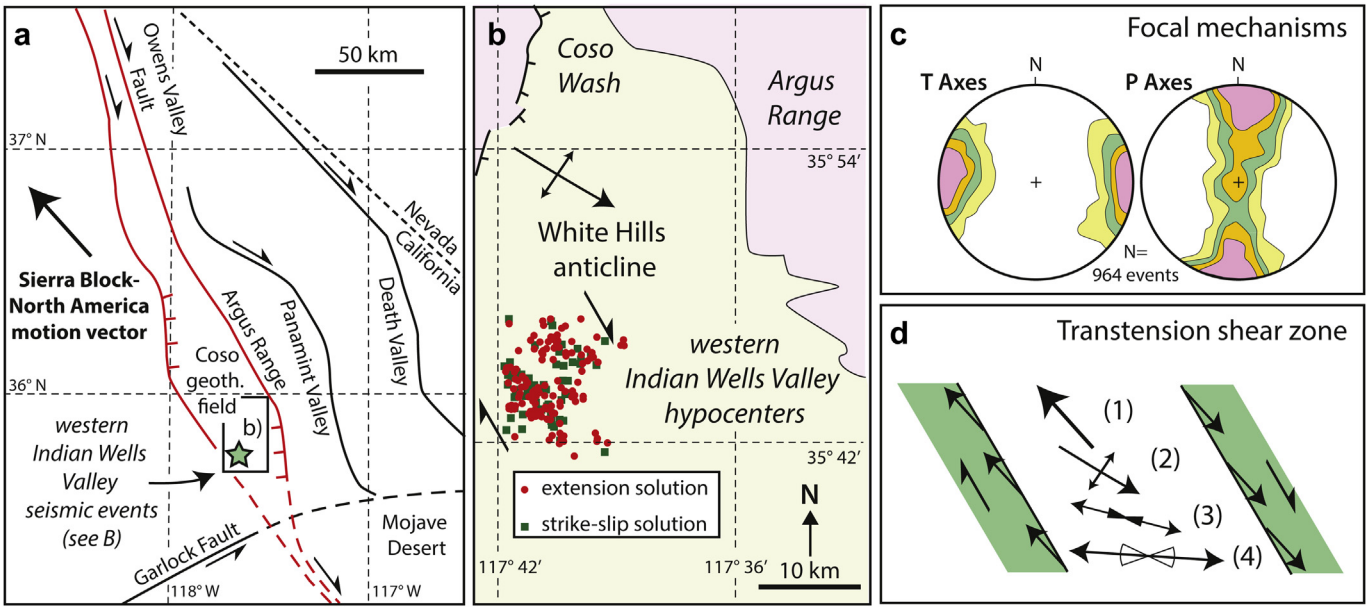

Fig. 14. Oblique divergence in Coso geothermal field, California. a) Simplified map of active faults in the Eastern California-Walker Lane shear zone, between the Sierra Block and Death Valley, with location of Coso area shown in Fig. 14b. b) Hypocenters in the western Indian Wells Valley, with extension and strike-slip solutions distinguished; note White Hills anticline. c) P and T axes derived from seismic focal mechanisms (note girdle of P-axes, indicating horizontal to vertical shortening directions). d) Summary of strain and motion directions in Coso area (after Dixon et al., 2000 and Lewis, 2007a a & b: (1) Sierra Block-North America motion vector, (2) active fold axis, (3) GPS-determined stretching axis (based on 4 stations), (4) average T-axis determined from earthquake solutions.

8.3. Transtensional exhumation in the Western Gneiss Region (Norway)

The south-western part of the Scandinavian Caledonides is strongly influenced by post-collisional extension and strike-slip deformation (e.g., Johnston et al., 2007; Fossen, 2010), with a major steep Devonian shear zone, the Møre-Trøndelag shear zone (MTSZ), representing a zone of significant Devonian sinistral strike-slip deformation (Fig. 15). Immediately south of the western part of this shear zone are domains of ultrahigh-pressure rocks that have been exhumed from a depth in excess of 125 km (Van Roermund et al., 2002; Scambelluri et al., 2008). Supradetachment basins of Middle Devonian age, resting on the extensional Nordfjord-Sogn Detachment (e.g., Johnston et al., 2007; Vetti and Fossen, 2012), are folded into upright folds along with somewhat tighter folds and corrugations in the detachment zone (Chauvet and Séranne, 1994; Krabbendam and Dewey, 1998), whose E–W axial traces are portrayed in Fig. 15. The combination of exhumation, strike-slip and contemporaneous N–S shortening and E–W extension calls for transtension, and this part of the Western Gneiss Region with its overlying units has been interpreted as a zone of transtension with W_k increasing from south to north (Krabbendam and Dewey, 1998). Furthermore, strong linear fabrics (Fig. 16a) occur in much of the deformed part of the Western Gneiss Region along with Type 3 fold interference patterns (Fig. 16b) are also consistent with high-strain transtension.

Using the principles of transtensional folding discussed above, we can derive W_k from the angle ϕ between fold axes and the Møre-Trøndelag shear zone (Fig. 5). Transtensional fold hinges rotate toward a fixed oblique orientation α, which is that of the flow apophysis, or the direction of divergence. Depending on finite strain, the W_k values (Fig. 15) are minimum values because the folds are represented somewhere in the field between the two curves shown in Fig. 5, but closer to the lower curve than the upper one since the strains involved are relatively high. The data (Fig. 15) confirm that the amount of pure shear (low W_k numbers) increases to the south from Ålesund, and that the pure shear component may be higher in the ultrahigh-pressure domains between Ålesund and the Devonian Hornelen basin (Fig. 15). While folds in the shear zone itself are tight, folds in the lower Wk domain to the south are more open, consistent with the fact that pure shear-dominated transtension cannot produce tight folds. Hence the variation in fold

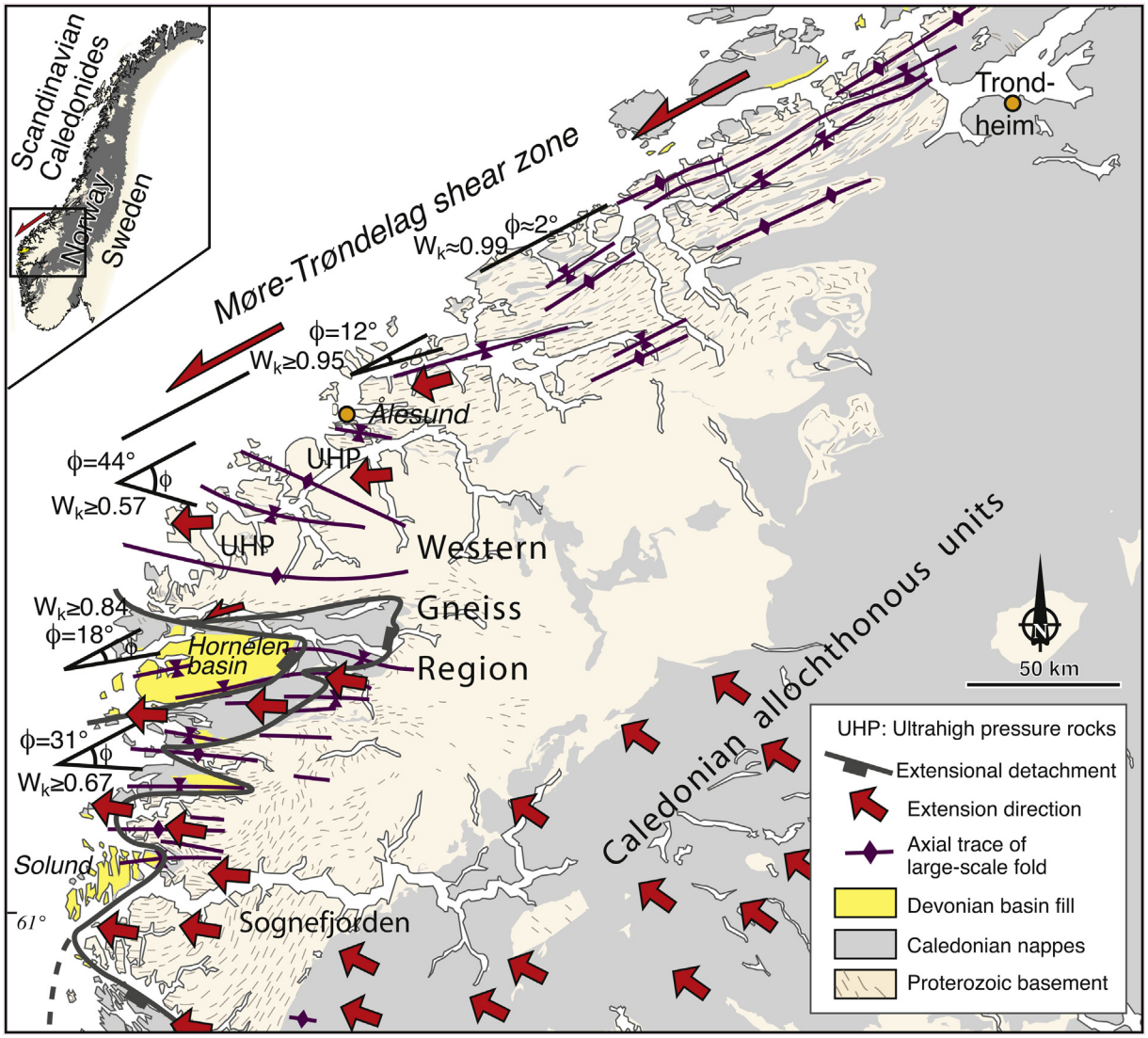

Fig. 15. Geologic map of the South Norway Caledonides. The angle ϕ between the Møre-Trøndelag shear zone and fold hinges is used to determine W_k using graph in Fig. 4a. Based on maps compiled by the Norwegian Geological Survey, Chauvet and Séranne (1994) and own field mapping and interpretations from remote sensing data.

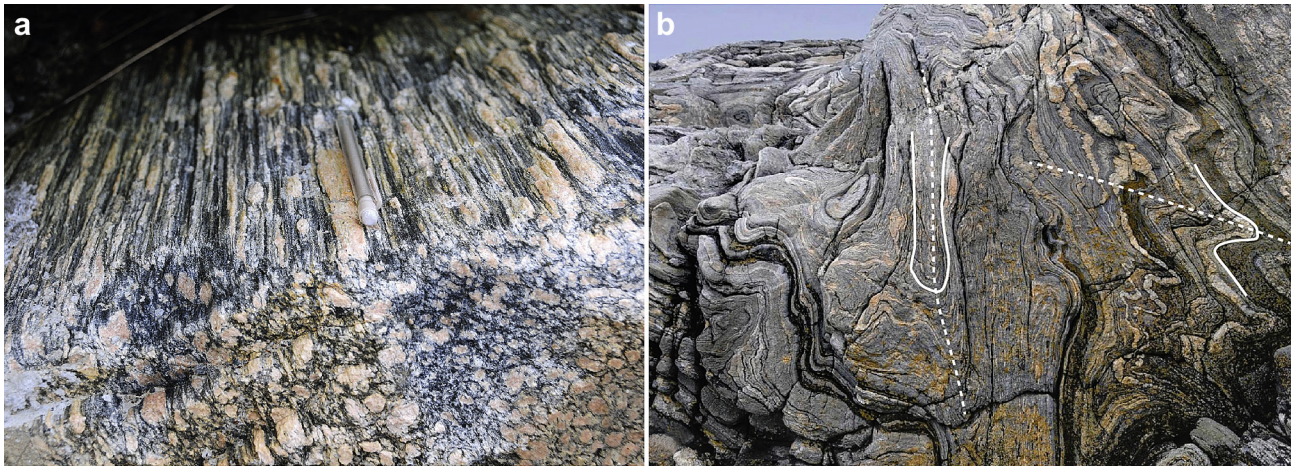

Fig. 16. a) Constrictional strain reflected by feldspar augen in granitic gneiss (Brattvåg). b) Banded gneiss folded by at least two sets of folds (steeply- and shallowly-dipping axial surfaces) (Ullaholmen). Both localities are located in the Møre-Trøndelag shear zone north-east of Ålesund).

geometry and orientation across this area is consistent with a variable type of transtension (changing W_k) (Krabbendam and Dewey, 1998).

9. Concluding remarks

The simple, monoclinic transtension model used in this study captures some important general characteristics of oblique divergence, including the fact that folds can form in the full range of transtensional deformations. Major results are as follows:

- The amount of shortening is dictated by the divergence vector or W_k, and while folds can amplify and tighten during simple shear-dominated transpression, only open folds are possible for pure shear-dominated transtension.
- Transtensional folds do not rotate toward the shear zone boundary, but rotate toward the orientation of the divergence vector. Therefore, the direction of transtensional fold hinges, in regions of high strain, is a good indicator of the direction of oblique divergence that generated the folds; transtension folds are expected to track relative plate motion in obliquely divergent plate boundaries.
- Transtensional folds are distinguished from folds formed during simple shear and transpression by their stronger hinge-parallel stretching and associated L-tectonite fabrics. In the brittle upper crust, normal/detachment faults as well as strike-slip faults develop to accommodate hinge-parallel stretching. In the ductile crust, hinge-parallel stretching and boudinage is prominent, while layers *in zone* around the fold hinges (fold limbs) undergo progressive shortening, commonly leading to fold interference patterns, owing to the constrictional nature of the flow.

As shown by the few examples treated here, the application of transtension theory to folding and stretching/boudinage is commonly problematic because any segment of deformed crust contains complex structures with a protracted, non-steady deformation history. However, the three-dimensional strain modeling presented here highlights the fact that steady oblique divergence potentially generates folds (for any angle of divergence), fold-interference patterns, and hinge-parallel stretching accommodated by brittle or ductile processes in a backdrop of overall constrictional strain. More generally, this work demonstrates that folds are expected to form in divergent tectonic settings; the signature of transtensional folds is the amount of syn-folding stretching that takes place in the direction parallel to fold hinges. These results highlight the necessity to analyze folds in three dimensions in order to derive useful information about the tectonic boundary conditions that generated the folds and associated structures and fabrics.

Acknowledgments

Thanks are due to Maarten Krabbendam and Steve Wesnousky for providing helpful reviews. Support from NSF grant EAR 1040980 is gratefully acknowledged.

References

Aragon-Arreola, M., Morandi, M., Martin-Barajas, A., Delgado-Argote, L., Gonzalez-Fernandez, A., 2005. Structure of the rift basins in the central Gulf of California: kinematic implications for oblique rifting. Tectonophysics 409, 19–38. http://dx.doi.org/10.1016/j.tecto.2005.08.002.

Chauvet, A., Séranne, M., 1994. Extension-parallel folding in the Scandinavian Caledonides: implications for late-orogenic processes. Tectonophysics 238, 31–54.

Corti, G., 2009. Continental rift evolution: from rift initiation to incipient break-up in the main Ethiopian Rift, East Africa. Earth-science Reviews 96, 1–53.

Dauteuil, O., Huchon, P., Quemeneur, F., Souriot, T., 2001. Propagation of an oblique spreading centre: the western Gulf of Aden. Tectonophysics 332, 423–442. http://dx.doi.org/10.1016/S0040-1951(00)00295-X.

Dixon, T.H., Miller, M., Farina, F., Wang, H.Z., Johnson, D., 2000. Present-day motion of the Sierra Nevada block and some tectonic implications for the Basin and Range province, North American Cordillera. Tectonics 19, 1–24. http://dx.doi.org/10.1029/1998TC001088.

Ehrhardt, A., Hubscher, C., Ben-Avraham, Z., Gajewski, D., 2005. Seismic study of pull-apart-induced sedimentation and deformation in the Northern Gulf of Aqaba (Elat). Tectonophysics 396, 59–79. http://dx.doi.org/10.1016/j.tecto.2004.10.011.

Fernandez, C., Diaz-Azpiroz, M., 2009. Triclinic transpression zones with inclined extrusion. J. Struct. Geol. 31, 1255–1269.

Fossen, H., 2010. Extensional tectonics in the North Atlantic Caledonides: a regional view. In: Law, R., Butler, R., Holdsworth, B., Krabbendam, R.A., Strachan, M. (Eds.), Geological Society of London Special Publication, vol. 335, pp. 767–793.

Fossen, H., Tikoff, B., 1993. The deformation matrix for simultaneous simple shearing, pure shearing, and volume change, and its application to transpression/transtension tectonics. J. Struct. Geol. 15, 413–422.

Fossen, H., Tikoff, B., 1998. Extended models of transpression/transtension and application to tectonic settings. In: Holdsworth, R.E., Strachan, R.A., Dewey, J.F. (Eds.), Continental Transpressional and Transtensional Tectonics, Geological Society of London Special Publication, vol. 135, pp. 15–33.

Fossen, H., Tikoff, B., Teyssier, C., 1994. Strain modeling of transpressional and transtensional deformation. Norsk Geol. Tidsskr. 74, 134–145.

James, A.I., Watkinson, A.J., 1994. Initiation of folding in wrench shear transpression. J. Struct. Geol. 16, 883–893.

Jamison, W.R., 1991. Kinematics of compressional fold development in convergent wrench terranes. Tectonophysics 190, 209–232.

Johnston, S.-M., Hacker, B.R., Andersen, T.B., 2007. Exhuming Norwegian ultrahigh-pressure rocks: overprinting extensional structures and the role of the Nordfjord-Sogn Detachment Zone. Tectonics 26, TC5001. http://dx.doi.org/10.1029/2005TC001933.

Jones, R.R., Holdsworth, R.E., Clegg, P., McCaffrey, K.J.W., Tavarnelli, E., 2004. Inclined transpression. J. Struct. Geol. 26, 1531–1548.

Krabbendam, M., Dewey, J.F., 1998. Exhumation of UHP rocks by transtension in the Western Gneiss Region, Scandinavian Caledonides. In: Holdsworth, R.E., Strachan, R.A., Dewey, J.F. (Eds.), Continental Transpressional and Transtensional Tectonics, Geological Society of London Special Publication, vol. 135, pp. 159–181.

Kruckenberg, S.C., Whitney, D.L., Teyssier, C., Fanning, C.M., Dunlap, W.J., 2008. Paleocene-Eocene migmatite crystallization, extension, and exhumation in the hinterland of the northern Cordillera: Okanogan dome, Washington, USA. Geol. Soc. Am. Bull. 120, 912–929.

Leroy, S., Razin, P., Autin, J., Bache, F., d'Acremont, E., Watremez, L., Robinet, J., Baurion, C., Denèle, Y., Bellahsen, N., Lucazeau, F., Rolandone, F., Rouzo, S., Kiel, J.S., Robin, C., Guillocheau, F., Tiberi, C., Basuyau, C., Beslier, M.-O., Ebinger, C., Stuart, G., Ahmed, A., Khanbari, K., Ganad, I., Clarens, P., Unternehr, P., Toubi, K., Lazki, A., 2012. From rifting to oceanic spreading in the Gulf of Aden: a synthesis. Arab. J. Geosci. 5, 859–901. http://dx.doi.org/10.1007/s12517-011-0475-4.

Lewis, J.C., 2007a. Fine-scale partitioning of contemporary strain in the southern Walker Lane: Implications for accommodating divergent strike-slip motion. J. Struct. Geol. 29, 1201–1215.

Lewis, J.C., 2007b. Multiple constraints on divergent strike-slip deformation along the eastern margin of the Sierran microplate, SE California. Geol. Soc. Am. Spec. Papers 434, 107–128.

Lonsdale, P., 1989. Segmentation of the Pacific-Nazca spreading center, 1-DEGREES-N-20-DEGREES-S. J. Geophy. Res.-solid Earth 94 (B9), 12197–12225. http://dx.doi.org/10.1029/JB094iB09p12197.

Mart, Y., Ryan, W.B.F., Lunina, O.V., 2005. Review of the tectonics of the Levant Rift system: the structural significance of oblique continental breakup. Tectonophysics 395, 209–232. http://dx.doi.org/10.1016/j.tecto.2004.09.007.

McFadden, R.R., Siddoway, C.S., Teyssier, C., Fanning, C.M., 2010. Cretaceous oblique extensional deformation and magma accumulation in the Fosdick Mountains migmatite-cored gneiss dome, West Antarctica. Tectonics 29, TC4022.

McNeill, L.C., Mille, A., Minshull, T.A., Bull, J.M., Kenyon, N.H., Ivanov, M., 2004. Extension of the North Anatolian Fault into the North Aegean Trough: evidence for transtension, strain partitioning, and analogues for Sea of Marmara basin models. Tectonics 23, TC2016. http://dx.doi.org/10.1029/2002TC001490.

Mortimer, E., Paton, D.A., Scholz, C.A., Strecker, M.R., Blisniuk, P., 2007. Orthogonal to oblique rifting: effect of rift basin orientation in the evolution of the North basin, Malawi Rift, East Africa. Basin Res. 19, 393–407.

Nagy, E.A., Stock, J.M., 2000. Structural controls on the continent-ocean transition in the northern Gulf of California. J. Geophys. Res.-solid Earth 105 (B7), 16251–16269. http://dx.doi.org/10.1029/1999JB900402.

Nicolas, A., Bouchez, J.-L., Blaise, J., Poirier, J.-P., 1977. Geological aspects of deformation in continental shear zones. Tectonophysics 42, 55–73.

Oskin, M., Stock, J.M., Martin-Barajas, A., 2001. Rapid localization of Pacific-North America plate motion in the Gulf of California. Geology 29, 459–462. http://dx.doi.org/10.1130/0091-7613.

Ramsay, J.G., Huber, M.I., 1983. The Techniques of Modern Structural Geology: Strain Analysis. Academic Press, London.

Ramsay, J.G., Huber, M.I., 1987. The Techniques of Modern Structural Geology: Folds and Fractures. Academic Press, London.

Rey, P.F., Teyssier, C., Kruckenberg, S.C., Whitney, D.L., 2011. Viscous collision in channel explains double domes in metamorphic core complexes. Geology 39, 387–390.

Robin, P.-Y.F., 1994. Strain and vorticity patterns in ideally ductile transpression zones. J. Struct. Geol. 6, 447–466.

Rosendahl, B.R., 1987. Architecture of continental rifts with respect to East Africa. Ann. Rev. Earth Planet. Sci. 15, 445–503.

Sanderson, D., Marchini, R.D., 1984. Transpression. J. Struct. Geol. 6, 449–458.

Scambelluri, M., Pettke, T., van Roermund, H.L.M., 2008. Majoritic garnets monitor deep subduction fluid flow and mantle dynamics. Geology 36, 59–62.

Seiler, C., Fletcher, J.M., Quigley, M.C., Gleadow, A.J.W., Kohn, B.P., 2010. Neogene structural evolution of the Sierra San Felipe, Baja California: evidence for proto-gulf transtension in the Gulf Extensional Province? Tectonophysics 488, 87–109.

Teyssier, C., Tikoff, B., 1998. Strike-slip partitioned transpression of the San Andreas fault system: a lithospheric-scale approach. In: Holdsworth, R.E., Strachan, R.A., Dewey, J.F. (Eds.), Continental Transpression and Transtensional Tectonics, Geological Society of London Special Publications, vol. 135, pp. 143–158.

Tikoff, B., Teyssier, C., 1992. Crustal scale, en échelon "P-shear" tensional bridges: a possible solution to the batholithic room problem. Geology, 927–930.

Tikoff, B., Teyssier, C., 1994. Strain modeling of displacement-field partitioning in transpressional orogens. J. Struct. Geol. 16, 1575–1588.

Tikoff, B., Fossen, H., 1993. Simultaneous pure and simple shear: the unified deformation matrix. Tectonophysics 217, 267–283.

Tikoff, B., Peterson, K.P., 1998. Physical experiments of transpressional folding. J. Struct. Geol. 20, 661–782.

Treagus, J.E., Treagus, S.H., 1981. Folds and the strain ellipsoid: a general model. J. Struct. Geol. 3, 1–17.

Umhoefer, P.J., Whitney, D., Teyssier, C., Fayon, A.K., Casale, G., Heizler, M., 2007. Yo-yo tectonics in a wrench zone, central Anatolia. In: Till, A.B., Roeske, S.M., Sample, J.C., Foster, D.A. (Eds.), Exhumation Associated with Continental Strike-slip Fault Systems, Geological Society of America Special Paper, vol. 434, pp. 35–57. http://dx.doi.org/10.1130/2007.2434(03).

Umhoefer, P.J., 2011. Why did the Southern Gulf of California rupture so rapidly? Oblique divergence across hot, weak lithosphere along a tectonically active margin. GSA Today 21 (11), 4–10. http://dx.doi.org/10.1130/G133A.1.

Van Roermund, H.L.M., Carswell, D.A., Drury, M., Heijboer, T.C., 2002. Microdiamonds in a megacrystic garnet websterite pod from Bardane on the island of Fjørtoft, western Norway: evidence for diamond formation in mantle rocks during deep continental subduction. Geology 30, 959–962.

Venkat-Ramani, M., Tikoff, B., 2002. Physical models of transtensional folding. Geology 30, 523–526.

Vetti, V., Fossen, H., 2012. Origin of contrasting Devonian supradetachment basin types in the Scandinavian Caledonides. Geology 40, 571–574.

Vigny, C., Socquet, A., Rangin, C., Chamot-Rooke, N., Pubellier, M., Bouin, M., Bertrand, G., Becker, M., 2003. Present-day crustal deformation around Sagaing fault, Myanmar. J. Geophy. Res.-Solid Earth 108. http://dx.doi.org/10.1029/2002JB001999.

Withjack, M.O., Jamison, W.R., 1986. Deformation produced by oblique rifting. Tectonophysics 126, 99–124.